Plasmonic resonances in ordered and disordered aluminum nanocavities arrays.

Plasmonic resonances in ordered and disordered aluminum nanocavities arrays.

R. G. Campuzano[1], **D. Mendoza**[2]
Instituto de Investigaciones en Materiales, Universidad Nacional Autónoma de México, 04510, Coyoacán, Ciudad de México.
E-mail: [1]naedra_9999@hotmail.com, [2]doroteo@unam.mx

Abstract. Nanocavities arrays were synthesized by electrochemical anodization of aluminum using oxalic and phosphoric acids as electrolytes. The morphology and topography of these structures were evaluated by SEM and AFM. Plasmonic properties of Al cavities arrays with different ordering and dimensions were analysed based on specular reflectivity. Al cavities arrays fabricated with phosphoric acid dramatically reduced the optical reflectivity as compared with unstructured Al. At the same time pronounced reflectivity dips were detectable in the 300nm-400nm range, which were ascribed to (0,1) plasmonic mode, and also a colored appearance in the samples is noticeably depending on the observation angle**.** These changes are not observed in samples made with oxalic acid and this fact was explained, based on a theoretical model, in terms that the surface plasmons are excited far in the UV range.

1. Introduction

Nano metallic objects derive their interesting optical properties from an ability to support collective electron excitations known as surface plasmons (SPs). Localized surface plasmon resonance (LSPR) confines light to nanostructures that are smaller than the wavelength of light, thereby enabling a family of novel plasmonic effects, such as extraordinary optical transmission (EOT) in subwavelength hole arrays **[1-4]** caused by a resonant coupling of light and surface plasmons.

In nanoscale systems, the plasmons of silver and gold (the most common plasmonic metals) are only tailored across the visible range, extending into the infrared regions and have their inherent drawbacks limits for extended applications **[5,6].** Contrastingly, the plasmons of Aluminum are tailored in the ultraviolet–visible–near-infrared (UV–vis–NIR) region of the electromagnetic spectrum. That is why it has been paid attention to this simple metal, because it possesses attractive properties including high natural abundance, low cost, high stability (because of the surface oxide layer); thereby making Al a promising alternative to conventional noble plasmonic materials. Recently, Al plasmonic has been increasingly used in studies and applications for its high performance as biosensors **[7]**, Surface Enhanced Fluorescence (SEF) **[8]**, and Surface Enhanced Raman Scattering (SERS) **[9]**.

In this work we present an electrochemical method **[10,11]** to fabricate regular and irregular arrays of aluminum concaves using oxalic acid and phosphoric acid, and their optical characterization by reflectance measurements. The main results are that plasmon resonances are excited in ordered as well

as in disordered array of concaves, and also the existence of colored appearance of the samples; the last result to our knowledge has not been reported yet.

2. Experimental details

High-purity aluminum foil (Sigma-Aldrich 0.25 mm thick, 99.999% purity) was cut in 1cmX2.5cm samples. Before the anodization process the Al foils were mechanically polished (mirror finish) and ultrasonically degreased in deionized water, acetone and ethanol and subsequently electropolished in a 1:4 mixture of 70% $HClO_4$ and 96% CH_3CH_2OH at a constant voltage of 18V for 2 min at 3 ºC. Two kinds of samples using oxalic and phosphoric acids as electrolytes for anodization were used. In one case, 0.3 M oxalic acid solution at 40 V for 7 h and for the second type, 0.1 M phosphoric acid solution at 130V and 160V at ambient temperature, and 150 V and 170 V at 3 ºC for 7 h were employed. A large aluminum plate (99.99% purity) was used as the counter electrode and the distance between both electrodes was kept 1cm apart, and the solution was continuously stirred to homogenize both the electrolyte and its temperature.

After anodizing, the samples were immersed in a mixture of 1.8 wt% CrO_3 and 6 wt% H_3PO_4 at 60 ºC for 12 h to selectively dissolve the anodic aluminum oxide (AAO), with this procedure an array of concaves is observed in the remaining aluminum surface. Morphology of the nanostructured aluminum samples and microanalysis of chemical composition was made using field-emission scanning electron microscope (SEM) JEOL 7600F FESEM equipped with energy dispersive X-ray spectrometer (EDS). Topography analysis was made with an Atomic Force Microscope JEOL Scanning Probe Microscope JSPM-4210.

To obtain geometrical parameters of the fabricated Al concaves Fast Fourier Transforms (FFTs) were generated based on SEM images using WSxM **[12,13]** and Image J software **[14]**. Reflectivity measurement was performed using UV-VIS Spectrophotometer (UV-2600 Shimadzu Corporation). The probe was set at normal angle and reflectance spectra were collected at 190-1400 nm wavelength range at an angle of 8 º. For comparison purposes, electropolished Al foil and Al film obtained by thermal evaporation were also measured.

3. Results and discussion

After anodization and thorough removal of the resulting AAO an array of concaves appear on the Al sample, which is an exact replica of the morphology of the AAO pore bottoms and their size depends on the applied voltage. SEM and AFM images of Al concave arrays fabricated in different electrolytes are shown in Fig. 1. The profiles show that the depths of the concavities made from phosphoric acid at 130V, 150 V, 160 V an 170 V were 210 nm, 250 nm , 310 nm and 360 nm respectively, and for oxalic acid was 20 nm.

To get better statistics on the geometrical parameters of Al concaves, the FFT analysis was performed on SEM images (Fig. 1). Based on FFT, the regularity ratio (RR) is a parameter that is related to the arrangement of concavities, which was estimated according to the following formula **[15]**:

$$RR = \frac{H}{W_{1/2}} \cdot n \tag{1}$$

where n is the number of concaves on the analyzed image, H the maximal intensity value of the FFT intensity profile, and $W_{1/2}$ is the width of the intensity profile at half of its height. The average interconcave distance (D_c) and pore concave diameter (D_d) were estimated from SEM images for each sample using Image J software. The determined values are presented in Table 1.

Table 1. Concave diameter (D_p), interconcave distance (D_c), regularity ratio (RR), and the wavelength where the minimum in reflectance appears (λ) values for the samples anodized with different acids.

Acid	Voltage (V)	Temperature	D_p (nm)	D_c (nm)	RR	](nm)
Oxalic	40	ambient	73.3±2.5	114.8±4.4	26.1±0.3	--
Phosphoric	130	ambient	240.9±12.6	357.1±4.4	25.3±0.9	317
Phosphoric	150	3 ºC	236.56±89.7	438.0±60.6	13.8±3.5	342
Phosphoric	160	ambient	353.2±27.3	417.1±18.6	25.98±1.6	371
Phosphoric	170	3 ºC	358.9±54.8	481.1±61.8	14.3±4.7	395

The FFT images of the samples fabricated at ambient temperature demonstrates six distinct points in the corners of a hexagon, confirming good hexagonal arrangement of concaves. In the case of the samples anodized at 3 ºC, the points in the FFT image are more blurred, suggesting lower degree of concaves order. In accordance with **[15,16]** the greater RR a better order in the arrangement of the concavities. As can be observed, the hexagonal concaves arrangement of the samples produced at ambient temperature is much better than the ones fabricated at 3 ºC, and this fact is reflected in the corresponding values of RR shown in Table 1.

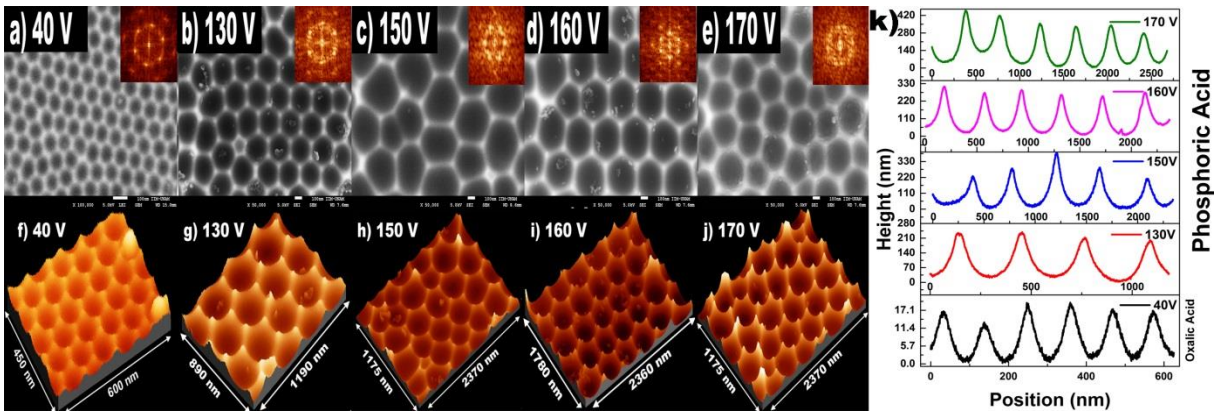

Fig. 1. SEM images of Al concaves fabricated using a) oxalic acid and b)-e) phosphoric acid with their respective FFT images (insets). AFM characterization of aluminum concaves in f) oxalic acid and g)-j) phosphoric acid. k) Concaves profiles obtained by AFM are shown for different acids.

Reflectance spectrum as a function of light wavelength of the Al nanoconcaves are shown in Fig. 2. Results for Al film obtained by thermal evaporation and electropolished aluminum are shown for comparison. A significant dip in the reflectivity intensity at 826 nm (~1.5 eV) is observed in all cases. This feature is related with interband transitions of electrons in the crystalline aluminum **[17,18]**. Additionally, a pronounced dip in the reflectivity in the 300nm-400nm range is observed in all the samples with concaves arrays obtained using phosphoric acid as the electrolyte. Note that the additional dip in the reflectivity of the sample made with oxalic acid does not appear within the worked spectral range.

The minima in UV region is a signature of SPs excitations **[19]**, which means that the incident light couples with surface plasmons located at Al concaves. The concave arrays provide the additional

momentum G necessary to fulfill the resonance conditions, giving rise to the dips in reflectivity spectra **[3, 19]**.

The surface plasmon resonances are directly associated with the periodicity of the concave arrays and to the optical properties of Al. At normal incidence, coupling of photons with 2-dimensional hexagonal periodic array gives SP resonances or minimum of the reflectivity at the wavelength given by **[3,20]**:

$$\lambda = \frac{P}{\sqrt{\frac{4}{3}(i^2 + ij + j^2)}} \sqrt{\frac{\varepsilon_m(\lambda)\varepsilon_d}{\varepsilon_m(\lambda) + \varepsilon_d}} \quad (2)$$

where P is the period of the array (in our case interconcave distance D_c), ε_m and ε_d are respectively the dielectric constants of the metal and the dielectric material in contact with the metal and i, j are the scattering orders of the array. Although the eq. (2) was developed for periodic arrays supporting SPPs resonances, to generate the SPPs a long-range order is not necessary; such as are shown in Fig. 2 for samples with disordered array of concaves.

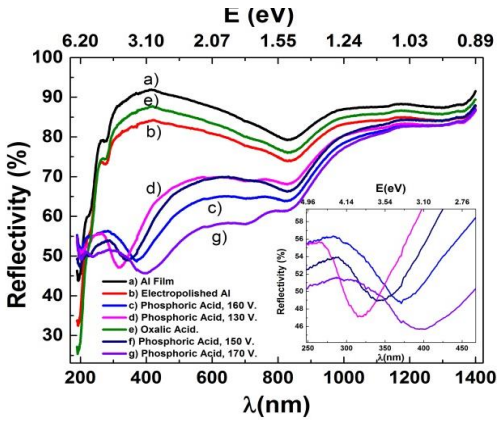

Fig. 2. Reflectivity spectrum of Al concaves fabricated with different acids. Results for electropolished Al foil and Al film obtained by thermal evaporation are shown for comparison.

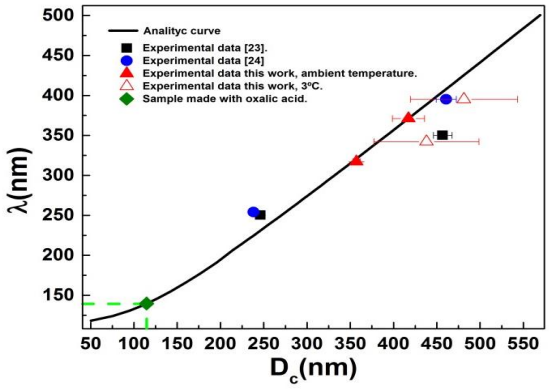

Fig. 3. Comparison of experimental data dip of this work and other works, and analytical curve for the surface plasmon resonance model for the fundamental mode (i, j)=(0,1). The green symbol marks the position for the wavelength where the dip in reflectance would locate for the sample made with oxalic acid.

Fig. 3 shows a comparison of experimental data of the reflectivity dip observed in this work and reported in other works **[23,24]**, and theoretical curve for the surface plasmon resonance model with periodicity described by Eq. (2)**.** For calculations, Eq. 2 was solved using experimental values for the dielectric function of aluminum $\varepsilon_m(\lambda)$ **[21,22]** and taking $\varepsilon_d = 1$ for air. Experimental data of the samples made with the conditions here presented and also for data reported for other authors fit well with the theoretical curve. Note that the results for the samples with a disordered array of concaves are also well reproduced by the theoretical model, which may be interpreted as that the periodicity is not essential for the excitation of surface plasmons and that the irregularity on the surface is the important characteristic for the momentum conservation rule. As a predicting capability of the model, we can say that for the sample made with oxalic acid with interconcave distance of 114 nm, the plasmonic resonance would locate at a wavelength of around 139 nm; which is out of the experimental range of measurements, and this may be the reason for which no dip is observed for this kind of samples (see Figure 2).

The SPR model as shown in Eq. (2) is limited in that it does not account for variations in metal thickness or hole (concave) size. Resonant optical modes are known to shift to shorter wavelengths and decrease in bandwidth with increasing metal thickness **[4]**. It has also been shown that the resonant optical modes increase in magnitude, shift to longer wavelengths, and increase in bandwidth with an increase in hole size **[25].**

Finally, it is interesting to note that the samples made with phosphoric acid show a colored appearance depending on the observation angle, regardless the order in the concaves array, but not observed in the samples made with oxalic acid (see figure 4). Our hypothesis is that the surface plasmons decay radiatively emitting photons in the visible range in the case of samples made with phosphoric acid, and in the far-UV range for the samples made with oxalic acid; this process because the strong coupling of plasmons and photons through the irregularities on the aluminum surface **[19]**. But this observed phenomenon deserves further careful investigation.

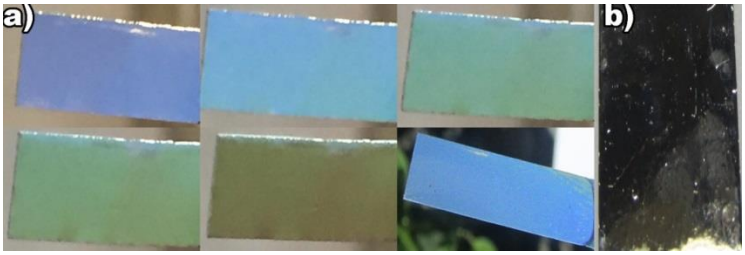

Fig.4. Colored appearance of samples anodized with a) phosphoric acid for different angles and b) oxalic acid.

4. Conclusión

Aluminum concave arrays were prepared by electrochemical anodization using oxalic and phosphoric acid as electrolytes. Geometrical order was determined by FFTs analysis. Plasmonic properties of Al arrays of concaves with different periodicities and dimensions were analyzed based on reflectivity measurements. It was found that, regardless the periodicity, the arrays of Al concaves obtained with phosphoric acid dramatically change the optical reflectivity of the surface compared with flat unstructured Al surface. The modified aluminum surface present a pronounced reflectivity dip as well as a colored appearance. These changes are not observed in samples made with oxalic acid and were explained, based on a theoretical model, in terms that the surface plasmons are excited far in the UV range. The order and geometrical dimensions of the concaves can be simply changed by manipulation of operational parameters, such as voltage, temperature or anodization time.

Acknowledgements. We thank Josue Esau (SEM), Carlos Flores (AFM), M. A. Canseco (UV-Vis) for their valuable assistance and Prof. E. Geffroy for kindly providing us with deionized water, all them at IIM-UNAM.

5. References

[1] Ebbesen T W 1998, et. al. *Nature* **391** 667-9.
[2] Coe J V, Heer J M 2008, et. al. *Annu. Rev.Phys.* Chem. **59** 179–202.
[3] Genet C, Ebbesen T W 2007 Light in tiny holes. *Nature* **445** 39–46.
[4] Martín-Moreno L 2001, et. al. *Phys. Rev*. Lett. **86** 1114–17.
[5] Samuel E and Lohse 2014, et. al. *Chem. Mater*. **26** 34–43.
[6] Matthew N O'Brien 2014, et. al. J. *Am. Chem. Soc*. 136 (21) 7603–06.
[7] Wanbo Li 2016, et. al. *Biosensors and Bioelectronics* 79 500–7.
[8] Mustafa H. Chowdhury 2009, et. al. *Anal. Chem*. 81 (4) 1397–1403
[9] Xiaoyu Zhang 2006. et. al. *J. Am. Chem. Soc*. 128 (31) 10304–09.
[10] Hideki Masuda 1995, et. al. Science **268** 1466-68.
[11] Sousa C T 2014, et. al. *Applied Physics Reviews* **1**, 031102

[12] Horcas I 2007, et. al. Rev. Sci. Instrum. 78 8, 013705.
[13] WSxM, http://www.wsxmsolutions.com/
[14] ImageJ, https://imagej.nih.gov/ij/
[15] Wojciech J. 2011 et. al. *Surf. Coat. Technol*. **206** 1416–22.
[16] Wojciech J and Stępniowski.2014 et. al. Materials Characterization. **91** 1–9.
[17] Hughes A. 1969 et. al. *J. Phys. C: Solid State Phys*. **2**, 102.
[18] H. Ehrenreich 1963 et. al. *Phys. Rev*. **132** 1918-28.
[19] Heinz Raether 1988 Surface Plasmons on Smooth and Rough Surfaces and on Gratings. Springer
[20] Tracts in Modern Physics, Vol. 111, Springer Berlin
[20] E.T. Papaioannou, et. al. Opt. Express 19 (2011) 23867-877.
[21] Rakic A D 1998, et. al. *Appl. Opt.* **37** (5271-83.
[22] Weaver J H, et. al. Optical Properties of Metals II: Noble Metals, Aluminum, Lanthanides, and Actinides, 0.1-500 eV, Zentralstelle für Atomkernenergie-Dokumentation, ZAED, 1981, 320 pp.
[23] Małgorzata Norek 2014, et. al. Current Applied Physics **14** 1514-20.
[24] Małgorzata Noreka, 2014 et. al. *Applied Surface Science* **314** 807–14.
[25] Van Der Molen K L 2004, et. al. Appl. Phys. Lett., **85** 4316–18.